THE JOURNAL OF PHYSICAL CHEMISTRY A

Article

pubs.acs.org/JPCA

Molecular Models of Cesium and Rubidium Adsorption on Weathered Micaceous Minerals

Laura K. Zaunbrecher,[†] Randall T. Cygan,[‡] and W. Crawford Elliott*[,†]

[†]Department of Geosciences, Georgia State University, Atlanta, Georgia 30302-3965, United States

[‡]Geochemistry Department, Sandia National Laboratories, Albuquerque, New Mexico 87185-0754, United States

ABSTRACT: Understanding the adsorption mechanisms of metal cations onto soils and sediments is of critical importance in the protection of the environment, especially for the case of radioactive materials including the fission product ^{137}Cs. Mechanism-based adsorption models for the long-term interaction of chemical and radionuclide species with clay minerals are needed to improve the accuracy of groundwater reaction and flow models, as well as related simulations for performance assessment of waste sites and repositories. Toward this goal, molecular simulation using geometry optimization and molecular dynamics methods have been used to investigate the adsorption behavior of Cs^+ and Rb^+ cations at frayed edge wedges (a proxy for frayed edge sites, FES) and in the interlayer region formed as a result of the transformation of muscovite to Al-hydroxy interlayered vermiculite (HIV) during weathering and pedogenesis. Frayed edge wedges, formed both on individual smectite and illite phases and on the mica-HIV intergrade, have previously been recognized as significant sinks for the strong adsorption of Cs^+ and Rb^+. Atomic density profiles, interlayer adsorption site maps, radial distribution functions, and adsorption enthalpies derived from the equilibrated structural models are used to evaluate the optimal adsorption configurations and thermodynamics for Cs- and Rb-endmembers, a 50:50 Cs−Rb composition for the aqueous interlayer of vermiculite, and for the interlayer wedge zone as mica is transformed to HIV (i.e., HIV-mica wedge). Adsorption enthalpies for both cations are significantly larger for the frayed edge wedges (as represented by the HIV-mica wedge model) compared to values for the vermiculite and mica interlayers. Cesium cation binds more strongly than Rb^+ in the vermiculite interlayer, while Rb^+ binds more strongly than Cs^+ in the HIV-mica wedge. In all cases, the derived adsorption enthalpies for both cations indicate a preference for the wedge environment where electrostatic interaction is enhanced due to the presence of layer charge and the increased size of interlayer at the wedge accommodating cations larger than K^+.

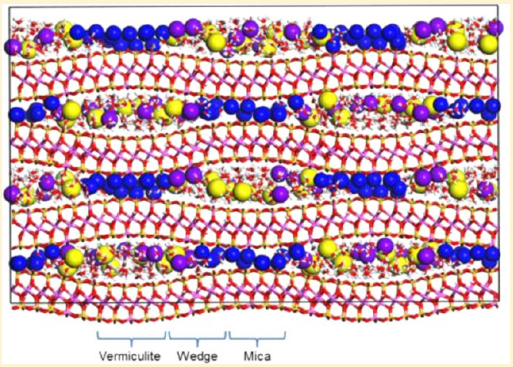

INTRODUCTION

The adsorption of cesium ions and related alkali and alkaline earth metals on mineral phases in soils (illite, in particular) has been described by many investigators at many study areas. Radioactive Cs (^{137}Cs) and stable Cs are adsorbed effectively by micaceous minerals, particularly illite in soils and sediments per many studies conducted during the past 50 years.[1−9] In these and many other studies, ^{137}Cs and stable Cs were found adsorbed at one or more of three possible locations in muscovite and illite grains (planar surfaces, edges, and within interlayer wedges exposed at frayed edges). The Cs^+ adsorbed on phyllosilicate mineral surfaces and many interlayer sites is readily exchangeable. However, Cs^+ is adsorbed more strongly at the frayed edge sites (FES) found within wedges developed as muscovite or illite layers are splayed from each other during weathering, as described by Jackson.[8] The FES found within these splayed layers (i.e., wedges) are highly selective for Cs^+ over aqueous cations of other major elements.[2,10,11] The FES develop as the 2:1 layers of the parent illite or muscovite splay apart from each other during weathering. As the phyllosilicate mineral layers become frayed, K^+ originally fixed in the interlayers is removed and replaced by other cations from the soil solution.[12] Cesium held strongly in FES within the frayed edge wedges (i.e., frayed wedges or wedges) is resistant to cation exchange with radioactive Cs or Rb.[6] The number of these highly Cs-selective frayed edge sites is low (less than 2%) in illite and mica.[10,13] The distribution coefficients for Cs^+ adsorption by illite of widely varying geologic age are positively correlated with the surface area of the frayed edges further demonstrating the effect of these FES on the adsorption of Cs^+ from solution.[14]

In addition to the well-known FES of illite, a related adsorption environment for alkali metals exists in the interlayer regions of highly weathered particles that once were muscovite but now are mostly Al-hydroxy interlayered vermiculite (HIV).[15] In many highly weathered soils (e.g., ultisols), parent muscovite and illite have been transformed mostly to HIV by chemical weathering leaving remnants of muscovite.[16−20]

Received: December 23, 2014
Revised: March 11, 2015
Published: April 23, 2015

DOI: 10.1021/jp512824k
J. Phys. Chem. A 2015, 119, 5691−5700

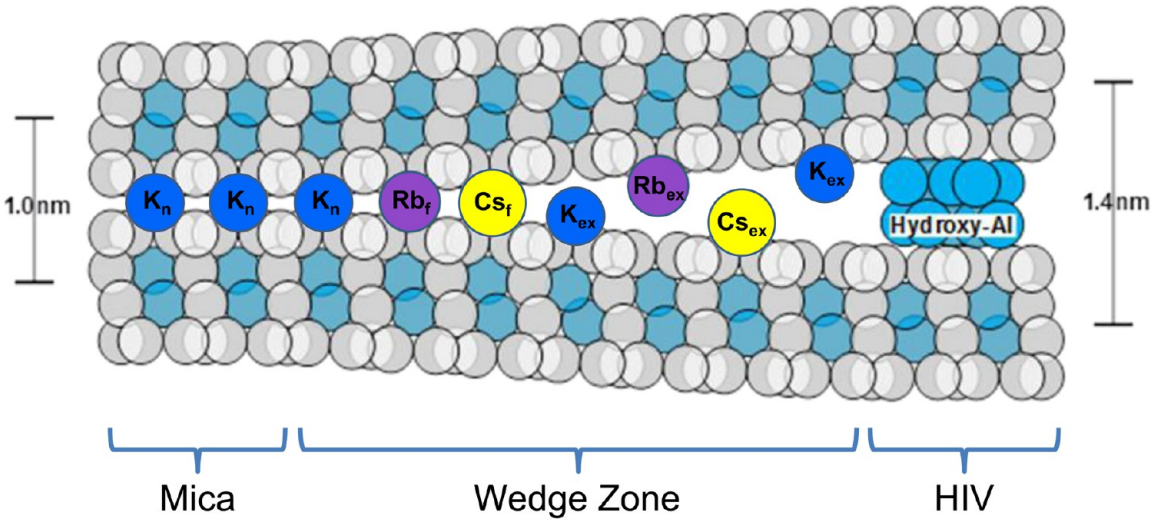

Figure 1. Conceptual view of two phyllosilicate layers comprising mica, vermiculite (HIV), and the wedge zone between mica and HIV in cross-section. This view shows a conceptualization of the transformation of mica to HIV. The fixation of Rb_f and Cs_f is found toward the apex of the wedge zone where subscript f denotes Rb and Cs ions effectively fixed within the layers near the apex of the wedge. K_n denotes native K^+ in mica. Subscript ex denotes exchangeable ions. Oxygen atoms are represented by light gray circles and hydroxyl ions by light blue circles. All Cs^+, Rb^+, and K^+ are located in the center of ditrigonal cavities found in the basal surface of oxygen atoms (siloxane sheet) at the base of the two phyllosilicate layers. Water molecules, silicon atoms, and aluminum ions are not represented. Modified from Wampler et al.[7]

Aluminum-hydroxy polymers are precipitated between the layers producing HIV.[16,21] The transformation of mica to HIV is known well in the U.S. Atlantic Coastal Plain soils and Piedmont province in the SE United States.[17,18] HIV is found in volcanic soils in Japan.[22,23] HIV grains are known to adsorb radioactive Cs (^{137}Cs) based on studies from the U.S.,[4,6,24] Japan,[22] and Belgium.[19] Recent work from the Savannah River Site (SRS) shows that HIV grains with occluded muscovite remnants have adsorbed relatively large amounts of natural (nonradioactive) Cs, both in surface soils and in soils at depth.[7,25] The foregoing work shows the adsorption and lack of exchange of adsorbed Cs^+ in FES associated within the frayed edge wedge formed between mica and vermiculite (or Al-hydroxy HIV). These studies also show the adsorption of Cs^+ in frayed edge wedges and in the adjacent interlayer formed where muscovite has transformed to HIV. The results lead to a conceptual view of the adsorption of Cs^+ and Rb^+ in interlayer and wedge sites. The wedges are formed as muscovite mica is transformed into HIV through soil weathering processes. Rubidium and Cs^+ are fixed strongly near the apex of the wedge formed as the layers are splayed from each other (Figure 1).

The above conceptual view results from exchange experiments coupled with results characterizing the clay fractions. At the atomic scale, Cs^+ is adsorbed strongly as inner sphere adsorption complexes centered in the ditrigonal cavity in the siloxane plane at wedge sites relative to outer sphere adsorption complexes for most other cations in interlayer sites.[9,26,27] This adsorption of Cs^+ as an inner sphere complex is resistant to ion exchange, and the adsorption of Cs^+ may result in partial collapse of the frayed 2:1 phyllosilicate layers around Cs^+, causing the adsorbed Cs^+ to be resistant to further exchange.[6,7,26,27] The adsorption of Cs^+ in FES is dependent on the clay mineral content in the soil and Cs^+ adsorption may be inhibited by the presence of natural organic matter.[28,29]

Molecular simulation has been used to understand further the adsorption of radionuclides on soil minerals.[9,30,31] For example, the application of classical molecular dynamics has been used to study the adsorption of various metal cations (Pb^{2+}, Cs^+, Na^+, Cd^{2+}) on kaolinite surfaces, resulting in new information regarding the type of adsorption of these metals either as strong inner sphere complexes centered on ditrigonal cavities on the siloxane mineral surfaces or as outer sphere complexes.[32] Quantum and electronic structure calculations based on density functional theory have been used recently to investigate the structure of interlayer Cs^+ in illite.[9] Molecular simulation methods can be used to determine the metals adsorbed with the lowest energy configurations (enthaplic energies). The molecular configuration with the lowest free energy is likely the most stable structure. Of interest to this study, molecular models are constructed to simulate the adsorption of different metal cation (Cs^+ and Rb^+) on a constructed frayed edge model to determine the energetically favored metal cation (Cs^+, Rb^+, or a mixture of Cs^+ and Rb^+). The molecular simulations are used to derive the structure of the aqueous interlayer of vermiculite and the HIV-mica wedge, and the thermodynamics of cation adsorption in these clay mineral models.

METHODS

Molecular dynamics (MD) simulations were performed using models of various layered aluminosilicate structures representative of dioctahedral vermiculite and representative of a frayed edge wedge zone formed between HIV and mica intergrade (Figure 1). Periodic models of a wedge zone effectively represent the structural environment associated with a FES in a mica-vermiculite intergrade, as shown in Figure 1. A dioctahedral vermiculite structure was initially developed from the uncharged layer structure of pyrophyllite ($Al_2Si_4O_{10}(OH)_2$)[33] using random substitution of Al for Si in the tetrahedral sheets. The short-range ordering of the Loewenstein rule is imposed to avoid Al−O−Al linkages.[34,35] The subsequent hexagonal ring structure includes Si_6, Si_5Al, and Si_4Al_2 (*trans* only) structures. The resulting layer charge of −0.75 per $O_{10}(OH)_2$ unit is consistent with the layer charge expected for natural dioctahedral vermiculites.[36] Cesium and

DOI: 10.1021/jp512824k
J. Phys. Chem. A 2015, 119, 5691−5700

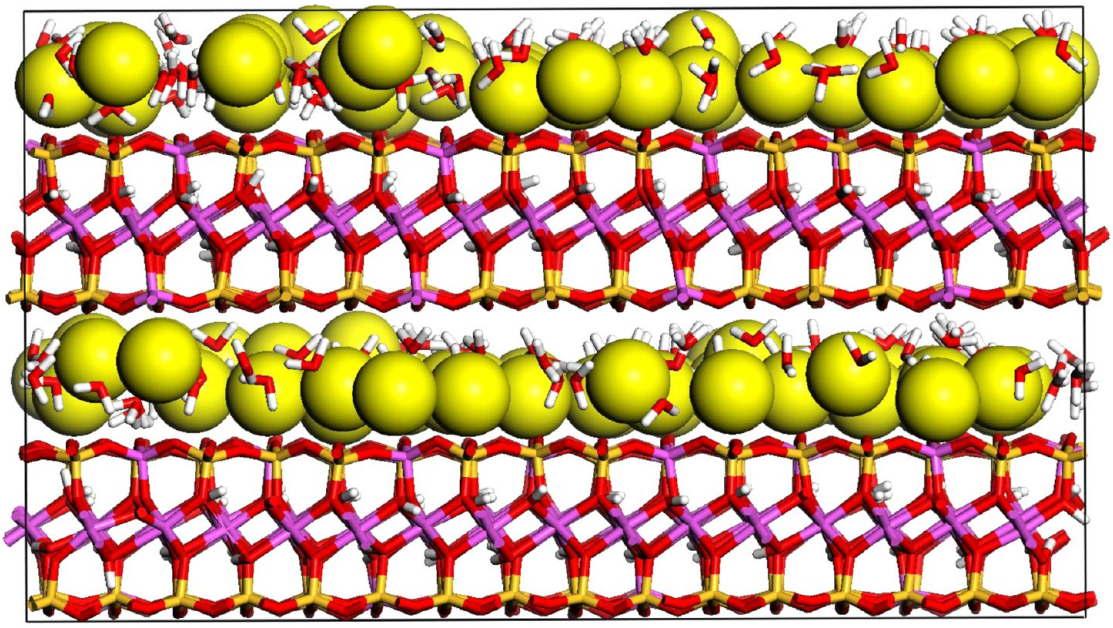

Figure 2. Equilibrated structure of Cs-vermiculite model derived from molecular dynamics. Cs^+ (yellow) and water molecules are observed in the interlayer.

rubidium cations were introduced at the midplane of the interlayer to balance the negative layer charge. Endmember models for each Rb, or Cs, plus an equal molar mixture of Rb and Cs were created. The vermiculite model has a nominal formula for the Cs endmember of $Cs_{0.75}(Si_{3.25}Al_{0.75})$-$Al_2O_{10}(OH)_2 \cdot 2H_2O$, where the water content represents a typical hydration state for a monolayer hydrate. Periodic orthogonal cells, with approximate dimensions of 41 Å × 36 Å × 25 Å, incorporated a total of 3412 atoms (including 252 water molecules) forming two clay layers and two interlayer regions (Figure 2).

Molecular model for the HIV-mica wedge intergrade structure has a novel structure created using a muscovite model[37] interlaced with the previously described vermiculite model. The initial hybrid model incorporated a two-layer dioctahedral phyllosilicate structure characterized by an alternating vermiculite region with two water layers, surrounded by a muscovite mica with −1.0 charge per $O_{10}(OH)_2$ unit ($KAl_2(Si_3Al)O_{10}(OH)_2$). The initial model was created by manually isolating large clusters of water molecules in the vermiculite interlayer section while maintaining a dry mica region. This structure was energy-optimized using an initially expanded interlayer and manually distorted clay layers to accommodate the transition between hydrate and dry water regions. Successive geometry optimizations while incrementally decreasing the *c*-dimension for an orthogonalized simulation cell produced a model with the characteristic wedge structure. Clay layer distortions involving extended bond distances were readily corrected by the optimizations using Clayff potentials (see below). After preliminary optimization of this initial structure (41 Å × 18 Å × 25 Å), the model was expanded to a 2 × 2 × 2 supercell with approximately 16 000 atoms, which was subsequently used for the large-scale molecular dynamics simulation of the HIV-mica wedge structure (see Figure 1). As prepared for vermiculite structure, endmember HIV-mica wedge models for Rb, Cs, and an equal mixture of Rb and Cs were created.

No hydroxylated Al^{3+} clusters are incorporated in the interlayer region of our wedge structural model due to lack of compatible Clayff parameters for interlayer Al. The periodic models of the wedge zone are supposed to effectively represent the structural environment associated with FES. The periodic model avoids explicit edge sites that would necessarily involve protonation−deprotonation reactions with an external aqueous solution and which can potentially affect access of aqueous cations to the clay interlayer. In this periodic case, the MD model provides a large number of replicated wedge sites to assess the exchange of cations. In contrast to the fully flexible models associated with the vermiculite simulations, the wedge model requires constrained clay layers which otherwise would relax, thereby destroying the wedge geometry and homogenizing the interlayer cation and water content.

Molecular dynamics simulations were conducted using the Large-scale Atomic/Molecular Massively Parallel Simulator (LAMMPS)[38,39] and Forcite[40] molecular simulation packages and the Clayff force field.[41] Clayff is a flexible energy force field that accurately describes the structure and energy of hydrated mineral systems using primarily nonbonded electrostatics and Lennard-Jones energy expressions derived from empirical and quantum mechanics methods. Bond-stretch and bond-angle energies for water molecules and bond-stretch energies for hydroxyls are evaluated using harmonic energy expressions associated with the SPC water model.[42] Energy parameters for Cs were taken from Clayff, based on the original work of Smith and Dang,[43] while the parameters for Rb were calculated from the interaction parameters reported by Åqvist.[44] Clayff does not reproduce accurately the ditrigonal distortion of the tetrahedral sheet[45] in the majority of phyllosilicate minerals.[41] In the following discussion, we refer to the sheet as having simply a hexagonal layer structure with Si(Al) rings and hexagonal holes.

Forcite-based simulations used an Ewald summation method[46,47] to evaluate long-range electrostatics to a precision of 0.0001, and a cutoff of 10.0 Å was used in evaluating the short-range Lennard-Jones interactions. A similar short-range cutoff was used for the LAMMPS simulations along with a

DOI: 10.1021/jp512824k
J. Phys. Chem. A 2015, 119, 5691−5700

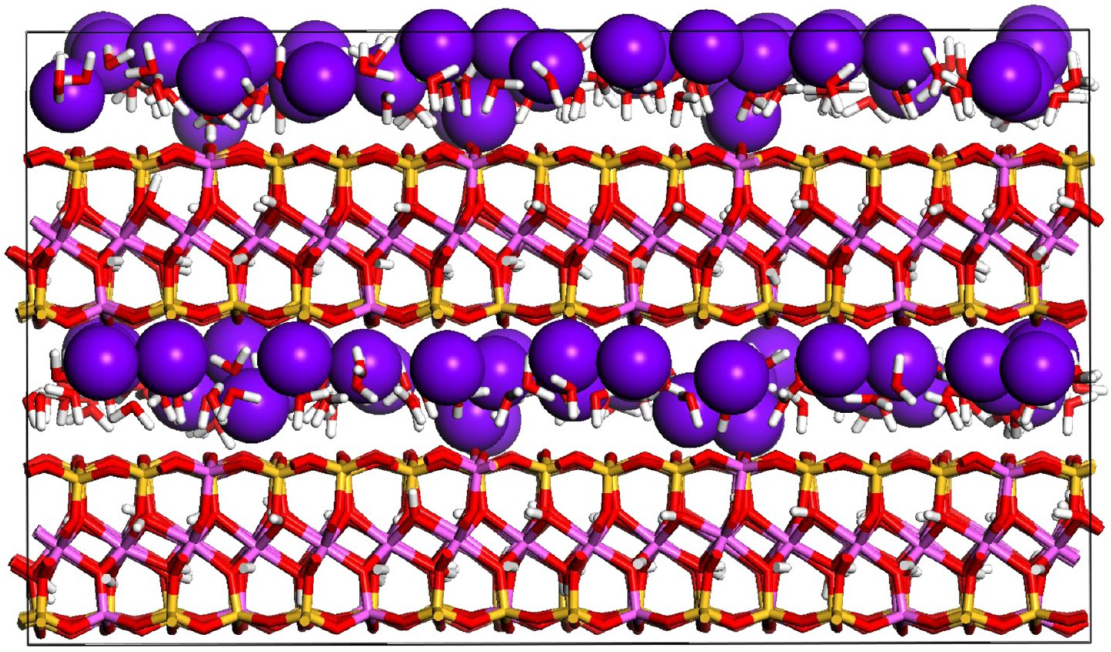

Figure 3. Equilibrated structure of Rb-vermiculite model derived from molecular dynamics. Rb^+ (purple) and water molecules are observed in the interlayer.

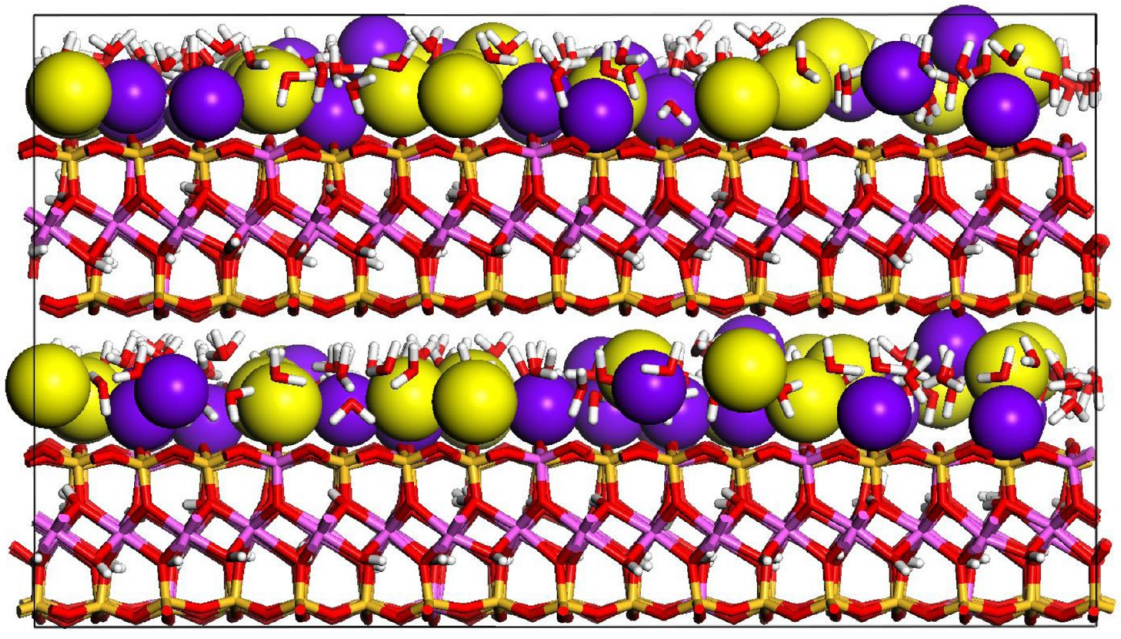

Figure 4. Equilibrated structure of mixed Cs−Rb-vermiculite model derived from molecular dynamics wherein Cs^+ (yellow), Rb^+ (purple), and water molecules are observed in the interlayer.

particle−particle particle−mesh for the electrostatics summation at a similar precision of 0.0001.[39] Molecular dynamics simulations employed a time step of 1 fs and a Nosé−Hoover thermostat and barostat[48] for equilibration at 300 K and 0.1 MPa (*NPT* ensemble). Initial simulations were completed to optimize the cell lengths while preserving the orthogonal nature of the simulation cell. Subsequent equilibration simulations used the canonical *NVT* ensemble for times up to 5 ns, while storing atomic trajectories every 500 fs over the final 1 ns of simulation time to represent the equilibrated structure. Atomic trajectories for the final 1 ns of each MD simulation are used to evaluate bulk structure, atomic profiles, Cs and Rb adsorption maps, and average adsorption structures. Potential energies derived from geometry optimizations of the initial 1 × 1 × 1 models of vermiculite and HIV-mica wedge structures, without interlayer water, were used for the determination of cation binding energies and adsorption enthalpies. Because of the need for constrained clay layers in the MD simulations of the wedge zone, only a canonical *NVT* ensemble was used.

RESULTS AND DISCUSSION

Dioctahedral Vermiculite. The bulk structure for the MD-equilibrated vermiculite model provides a basis for comparison of the adsorption of Cs^+ and Rb^+ onto the Al-substituted

DOI: 10.1021/jp512824k
J. Phys. Chem. A 2015, 119, 5691−5700

siloxane sheet of a high-charge phyllosilicate layer structure corresponding to dioctahedral vermiculite. Figures 2−4 provide snapshots of the equilibrated vermiculite structure for each of the three interlayer compositions (Cs, Rb, and mixed Cs−Rb composed of equal amounts of Cs and Rb). These vermiculite layers and interlayer water are identical for each of the MD simulations; only the interlayer cation compositions are different. Less than 0.07 Å difference is observed in the *c*-dimension for the *NPT*-equilibrated simulation cells for the three different interlayer compositions. The periodic boundary conditions imposed for the MD simulations ensure conserved atomic content across the simulation cell boundaries such that any cation or water motion across one boundary is immediately returned to the cell at the opposite cell boundary. Atoms in both interlayers, as represented in the simulation cell, are interacting directly with the vermiculite layer; the upper interlayer in the figures is bounded by a periodic image of the vermiculite layer on the bottom of the simulation cell.

Each system was initially equilibrated by the MD simulations which allow for the expansion or contraction of the interlayer region, hydration of the cations by coordinating water molecules, and the adsorption of cations or water molecules to the clay surface. For the Cs-vermiculite, a relatively broad distribution of both adsorbed Cs and water molecules are observed across the interlayer, with limited amounts of Cs and water directly adsorbed onto either of the clay siloxane surfaces (Figure 2). In contrast, for the Rb-vermiculite simulations, an asymmetrical distribution is seen of adsorbed Rb onto both siloxane clay surfaces with water molecules primarily distributed in the midplane of the interlayer. The mixed Cs−Rb vermiculite shows the competing adsorption of either cation onto the siloxane surfaces with limited water molecules directly adsorbed to the clay surface.

These adsorption behaviors of Cs^+, Rb^+, and equal mixture of Cs^+ and Rb^+ and vermiculite are more clearly displayed by the atomic density profiles across the two clay layers of the simulation cell as derived from the atomic trajectories (Figure 5). The profiles clearly exhibit the difference in atomic structure between the interlayer region and the vermiculite clay structure. The two T−O−T layers of the vermiculite are represented by structured Si, Al, and O peaks with Al peaks occurring in the central octahedral sheet and substituted in the Si tetrahedral sheet. There is an asymmetry (as shown in Figure 5) in the relative amount of Al substitution for Si in both clay layers that ultimately affects the interlayer structure. This asymmetry in tetrahedral Al is related to the randomization and disorder of sites during initial development of the vermiculite model. Hydrogen profiles associated with the octahedral hydroxyl group exhibit a tail that is influenced by both the dioctahedral vacancy and the charged site in the tetrahedral sheet. The interlayer regions for the Cs-vermiculite profile exhibit Cs^+ adsorbed preferentially to the siloxane surface where there is greater tetrahedral Al content. Inner-sphere adsorption also occurs to a lesser extent on the opposing clay surface. Both atomic density peaks for Cs^+ occur at equal distances on each side of the interlayer midplane. Water O_w is broadly distributed across the interlayer with water H_w. This water is located either in the midplane (water −OH parallel to the siloxane surface), or it is directly interacting with the siloxane O through hydrogen bonds.

Atomic density profiles for the Rb-vermiculite simulation are similar to those observed for Cs-vermiculite. The Rb-vermiculite exhibits a more ordered interlayer region. Rb^+

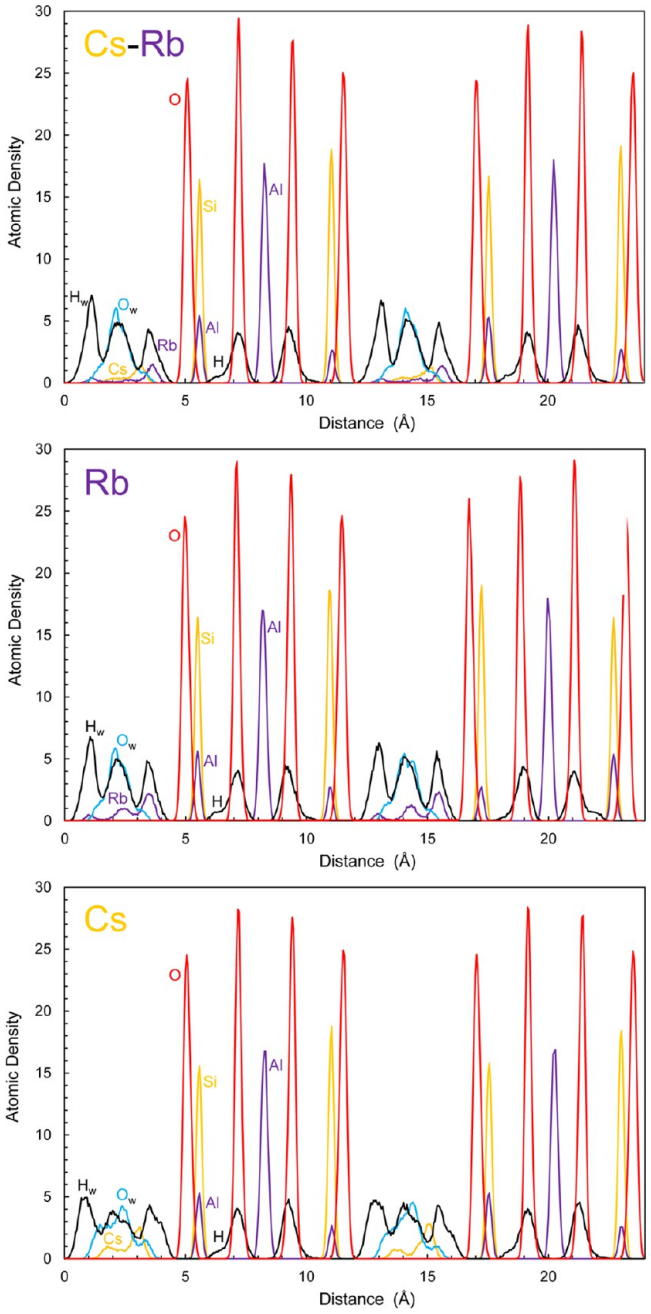

Figure 5. Atomic density profiles for the equilibrated endmember and mixed vermiculite models derived from molecular dynamics.

occurs across the interlayer in three interlayer configurations—from adsorbed to the low Al-substituted siloxane surface, to remaining in the midplane, to being preferentially adsorbed to the high Al-substituted siloxane surface. Water is more structured in the Rb-vermiculite interlayer region compared to that for Cs-vermiculite.

Results for the mixed Cs−Rb vermiculite, where competitive adsorption of the cations to the clay interlayer surfaces occurs, indicate almost equivalent adsorption of Cs^+ and Rb^+ to the high Al-substituted tetrahedral siloxane surface. Because of the ionic size difference between the two cations (Cs^+ = 1.78 Å and Rb^+ = 1.60 Å with coordination numbers of 9 and 8, respectively),[49] the atomic profiles indicate Rb^+ is adsorbed closer to the clay surface than Cs^+. The atomic profile is consistent with the snapshot image presented in Figure 4 for

DOI: 10.1021/jp512824k
J. Phys. Chem. A 2015, 119, 5691−5700

the Cs−Rb vermiculite. Visual inspection of Figure 4 indicates Rb^+ resides closer and more frequently than Cs^+ inside the hexagonal holes of the siloxane sheet. As observed for the endmember compositions, Rb^+ occurs in the midplane and sorbs to both clay surfaces. Cesium, on the other hand, avoids the low Al-substituted clay surface. Cesium typically is found more frequently than Rb^+ in the midplane region (Figure 4). The water structure represented by the H_w and O_w profiles is relatively ordered and is similar to that observed for the Rb-vermiculite (Figure 5).

The total atomic density profile for each of the vermiculite simulations does not discriminate among atomic components but represents the collective atomic structure (Figure 6). This profile representation simplifies the structural differences observed in the interlayer region among the more-diffuse behavior of the Cs model and the Rb and Cs−Rb models. From an experimental and spectroscopic perspective, the total atomic profile mimics data expected from X-ray reflectivity and coherent diffraction measurements,[50] but which to date have not been determined for phyllosilicate mineral systems.

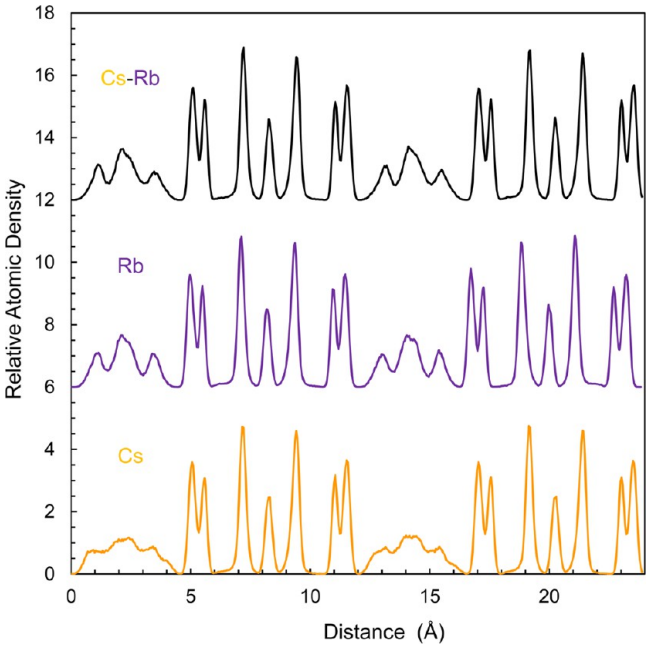

Figure 6. Total atomic density profiles for the equilibrated endmember and mixed vermiculate models derived from molecular dynamics.

Snapshot images of the equilibrated interlayer structures viewed normal to the hexagonal siloxane plane (relative to the high Al-substituted surface) are shown for each of the vermiculite simulations (Figure 7). Water molecules are typically observed either with H−O− bonds pointing toward the hexagonal ring or with water O coordinating to the interlayer cation. Cesium occurs predominantly at the hexagonal holes (73%) or coordinated to one or multiple bridging O (27%) in the Cs-vermiculite configuration. The number of Al substitutions, and corresponding charge sites, will affect cation binding at any particular hexagonal ring. For example, Cs^+ occurs adsorbed within both singly and doubly Al-substituted hexagonal rings. Rarely does Cs^+ adsorb immediately over an Al-substituted site. Net negative charge is highly localized at the Al-substituted site in the tetrahedral sheet. However, the charge is situated further away from the siloxane surface. The adsorption site directly in the hexagonal hole is closer to the localized charge at the Al-substituted site. The Rb-vermiculite exhibits 60% Rb^+ adsorbed within the hexagonal hole and 40% at or near bridging oxygens between tetrahedra. In part, this observation suggests that the smaller ionic size of Rb^+ is less than optimal for binding directly and symmetrically within the hexagonal ring structure. However, when Rb^+ does occur in the hexagonal hole, its ionic size allows it to bind closer to the tetrahedral sheet than Cs^+ (cf. Figure 4). The distribution of cations for the mixed Cs−Rb vermiculite shows the disposition of interlayer Cs^+ that is similar to that observed for endmember Cs. Similarly, Rb^+ distribution in the mixed Cs−Rb case is comparable to its distribution in the Rb vermiculite. Approximately 83% of the Cs and 67% of Rb occur symmetrically in the hexagonal hole. Although there is some influence of the opposing siloxane surface on the interlayer cation distribution, Rb cations, as noted previously, are engaged further into the hexagonal hole than Cs cations because of its smaller ionic size relative to Cs^+ (Figure 4).

HIV-Mica Wedge. The bulk periodic model for the HIV-mica wedge (a proxy for FES) structure provides a molecular basis to investigate compositional, charge distribution, and geometry effects on cation adsorption on a simulated frayed edge site. The large molecular model for the mixed Cs−Rb wedge is provided in Figure 8 (cf. conceptual model in Figure 1). All of the HIV-wedge models include a high-charge K-rich

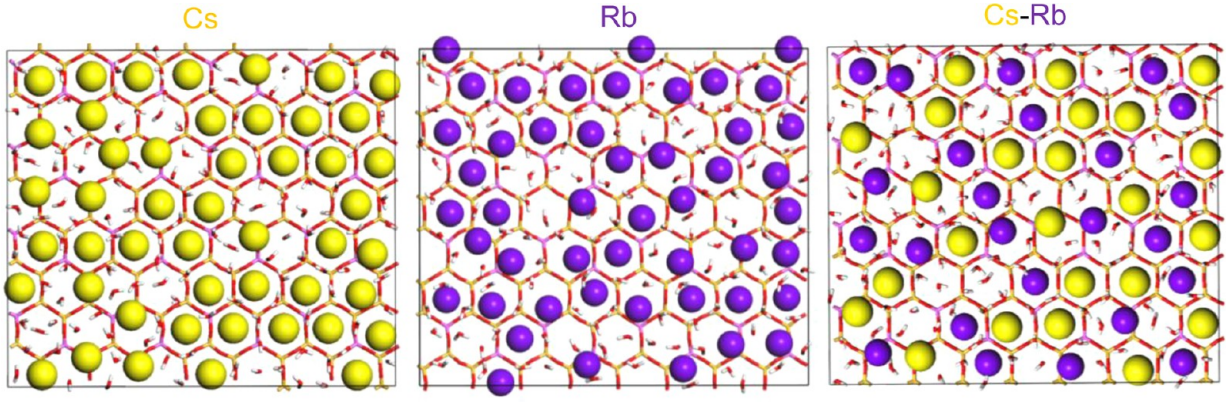

Figure 7. Distribution of Cs^+ (yellow) and Rb^+ (purple) in vermiculite interlayers relative to hexagonal silicate sheet and interlayer water derived from molecular dynamics. Al sites are indicated by magenta atoms in the stick representation of the hexagonal framework.

DOI: 10.1021/jp512824k
J. Phys. Chem. A 2015, 119, 5691−5700

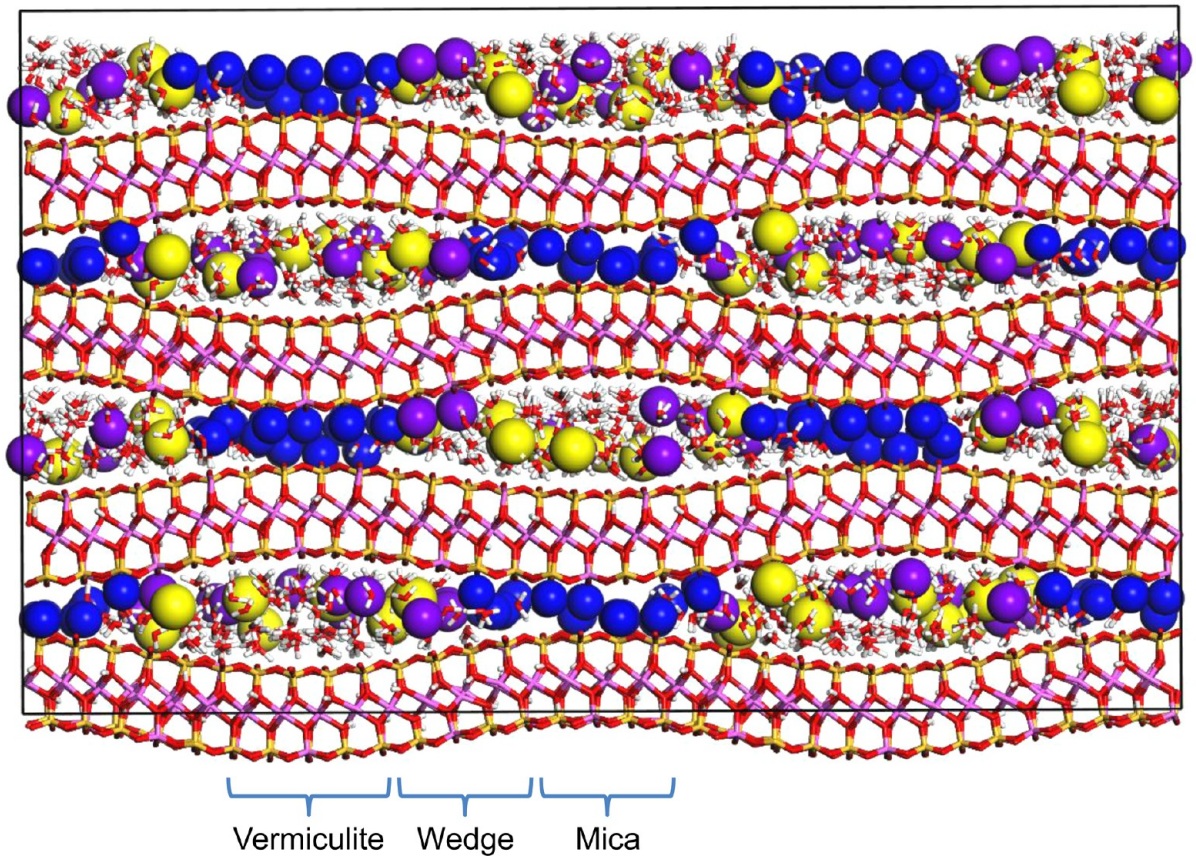

Figure 8. Equilibrated molecular structure of interlayer Cs^+ (yellow), Rb^+ (purple), and K^+ (blue) in mica-vermiculite hybrid structure (HIV-mica wedge model) as derived from molecular dynamics. Frayed edges are represented by wedge zone in periodic structure. Wedge, vermiculite, and mica zones are indicated for the lower left section of the simulation cell.

mica-like region combined with a hydrated Cs, Rb, or mixed Cs−Rb vermiculite region. The nature of the charge distribution between the collapsed mica region (−1.0 charge per $O_{10}(OH)_2$) and the hydrated vermiculite region (−0.75 charge per $O_{10}(OH)_2$) creates a complex competition between Cs^+ and Rb^+ for binding at the wedge site in the mixed Cs−Rb model. Similarly, there is an additional competition of the cations in the hydrated region where electrostatic adsorption of cations as inner-sphere complexes binding directly to the clay surface competes with the hydration of the cations by water molecules in the expanded interlayer region.

Equilibrated configurations from the MD simulations of the large 2 × 2 × 2 HIV-mica wedge models suggest a redistribution of the Cs^+ or Rb^+ in the vermiculite region from the initial uniform distribution for the endmember models. In both cases, during the equilibration stage of the simulation, the cations diffuse toward the wedge site and coordinate to the collapsed transition section of the wedge, typically shedding coordinating water molecules on the apex side of the wedge zone. Increased layer charge, associated with the Al-substituted siloxane sheets of the mica section, influences the enhanced binding of the cation while limiting the destabilizing effect of K−Cs and K−Rb repulsive interactions. Radial distribution function (RDF) analysis (not shown) of the equilibrated atomic trajectories suggests K−Cs and K−Rb interaction distances of 3.6 Å to 3.8 Å at the apex of the wedge site. Within the hydrated section of the structure (vermiculite zone), Cs^+ and Rb^+ interactions are influenced by the reduced layer charge and the distribution of the Al in the siloxane sheet. Although water molecules coordinate to the cations, there is strong interaction of Cs^+ and Rb^+ with the clay layers. Both cations form inner sphere complexes having mean RDF cation-siloxane O distances of 3.1 and 3.0 Å for, respectively, Cs^+ and Rb^+, and 3.0 and 2.9 Å for cation−water O distances. Similar interaction distances are observed for the mixed Cs−Rb HIV-mica wedge model as determined for the endmember cation simulations.

Cation Adsorption Energies. Analysis of the potential energy derived from the optimized structures of the dioctahedral vermiculite, mica, and HIV-mica wedge (1 × 1 x 1) models offers an opportunity to compare quantitatively the binding strengths for various interlayer cations. The difference in the average potential energies U provides a theoretical measure of the adsorption enthalpy ΔH_{ad}, as derived by the Clayff energy force field for each molecular system:

$$\Delta H_{ad} = \Delta U_{ad} + P\Delta V_{ad} \quad (1)$$

where

$$\Delta U_{ad} = \langle U_{clay\text{-}M} \rangle - \langle U_{clay} \rangle - \langle U_M \rangle \quad (2)$$

Knowing that the pressure P and volume difference ΔV terms for adsorption process associated with crustal sediment conditions are very small relative to the adsorption enthalpies, then the adsorption enthalpy is simply equal to the potential energy differences; that is, $\Delta H_{ad} = \Delta U_{ad}$. Also, the potential energy for an isolated nonsolvated cation U_M is by definition zero, which simplifies eq 2. In contrast, the adsorption enthalpy for a dry system ΔH_{dry} ignores any solvation effects and is often

DOI: 10.1021/jp512824k
J. Phys. Chem. A 2015, 119, 5691−5700

Table 1. Hydration Enthalpies for Solvated Cations and Adsorption Enthalpies for Interlayer Cations in Vermiculite, Mica, and HIV-Mica Models

	aqueous	vermiculite		mica		HIV-mica wedge	
	enthalpy (kJ/mol)						
interlayer cation	$\Delta H_{\text{M-hyd}}$[a]	ΔH_{dry}	ΔH_{ad}	ΔH_{dry}	ΔH_{ad}	ΔH_{dry}	ΔH_{ad}
Cs	−263	−424.9	−161.9	−719.8	−456.8	−518.6	−255.6
Rb	−296	−408.5	−112.5	−705.2	−409.2	−545.6	−249.6

[a]Burgess[51]

referred to as the binding energy of an adsorbate (e.g., cation). Knowing the hydration enthalpy for a cation $\Delta H_{\text{M-hyd}}$,[51] it is possible to correct this adsorption enthalpy ΔH_{dry} for the energy needed to extract the cation from its solvating water molecules and obtain a more accurate adsorption enthalpy:

$$\Delta H_{\text{ad}} = \Delta H_{\text{dry}} - \Delta H_{\text{M-hyd}} \quad (3)$$

Table 1 presents a comparison of the adsorption enthalpies for Cs^+ and Rb^+ interlayer cations in the vermiculite, mica, and wedge molecular models, along with the experimental hydration enthalpies for each cation. Adsorption enthalpies were derived for each of the dry molecular systems from the potential energy obtained from a geometry optimization calculation performed at constant pressure. A mica, with composition $M^+Al_2(Si_3Al)O_{10}(OH)_2$, was examined to provide a comparison of the vermiculite and HIV-mica wedge with a highly fixed environment for the two cations.

Based on the adsorption enthalpies under dry conditions, ΔH_{dry}, Cs^+ is favored energetically in the vermiculite and in the mica. For the hybrid wedge model, which is a representation of FES, Rb^+ exhibits a favored adsorption enthalpy in the wedge site for a dry model, although Cs^+ is the preferred adsorption cation after correcting for cation hydration. The differences in adsorption enthalpies, ΔH_{dry}, for the cations (16.4 kJ/mol in vermiculite, 14.6 kJ/mol in mica, and 27.0 kJ/mol in HIV-mica wedge) and the differences in adsorption enthalpy, ΔH_{ad}, with hydration correction (49.4 kJ/mol in vermiculite and 47.6 kJ/mol in mica) are significant, while ΔH_{ad} values for the cations in the HIV model are similar (only 6 kJ/mol difference) and may be sensitive to the variation observed in the published experimental hydration enthalpies for these cations.

The calculations for adsorption enthalpy suggest Cs^+ is likely to be more strongly bonded to the vermiculite phase, whereas Rb^+ is more strongly bonded to the interlayer wedge site (e.g., Rb_f, Figure 1) compared to Cs^+ (Cs_f, Figure 1), assuming the wedge model is an appropriate proxy for FES. The dry adsorption enthalpy, or binding energy, is the energy difference in having a cation at an optimized configuration relative to that with the cation at infinite separation. The adsorption enthalpy corrects the dry adsorption enthalpy for the enthalpy component associated with the cation being fully solvated by water molecules. Effectively, the binding energy represents the strength of the adsorption bond in the clay, and the adsorption enthalpy corresponds to the energy difference between the cation in solution and in a dry clay interlayer. All enthalpy values are negative and therefore represent a stabilization of the cation within the interlayer structure of the clay. Adsorption enthalpy values in Table 1 do not account for the partial hydration of adsorbed cations within the clay interlayer or wedge model, which could potentially lead to additional stabilization of the cation in the interlayer.

The dry adsorption enthalpies for both cations are greater for the FES, as represented by the HIV-mica wedge model, compared to adsorption in the vermiculite interlayer (more than 93 kJ/mol larger for Cs^+ and 137 kJ/mol larger for Rb^+). The corresponding enthalpies for cation adsorption in mica are much larger—more than 290 kJ/mol greater for both cations—than in vermiculite. Corrected adsorption enthalpies ΔH_{ad} for Cs^+ and Rb^+ are similarly larger for the wedge-based model (a proxy for FES) relative to vermiculite and for mica relative to vermiculite. The experimental values for the cation hydration enthalpies (Table 1) are in agreement with those derived from molecular dynamics simulations using the same interatomic potentials as in this study.[52]

Lastly, the total potential energies associated with the large HIV-mica wedge (2 × 2 × 2) simulations provide a complex composite of all atomic interactions associated with the interlayer region: cation−mica, cation−vermiculite, cation−wedge, cation−water, cation−cation, water−water. Nonetheless, the relative bulk adsorption energies of Cs^+ and Rb^+ can be determined. The Rb^+ endmember structure is more stable than the Cs^+ structure (by 33 ± 2 kJ/mol), while the potential energy for the mixed Cs−Rb (50:50) model is precisely intermediate between values the two endmember compositions.

CONCLUSION

For more than 50 years, the clay minerals community has invoked the concept of frayed edge sites to explain the enhanced adsorption behavior of smectite and illite phases for Cs^+ and other potentially hazardous metal cations. Because of the relatively long half-life of ^{137}Cs and its major presence in the environment after the 2011 Japanese earthquake and tsunami at the Fukushima nuclear power plant, there is renewed interest in better understanding the natural and engineered remediation of contamination by clay minerals. Additionally, significant ^{137}Cs contamination in the soils and sediments at the Savannah River Site in South Carolina (U.S.A.) has brought attention to the effectiveness of hydroxy interlayered vermiculite in removal of anthropogenic Cs from contaminated groundwaters. This study has attempted to present a molecular-based perspective on how Cs^+ and Rb^+—which is relatively common to the Savannah River Site and competes with Cs^+ in the soil phases—adsorb in vermiculite and the wedge structure of HIV (designed to mimic interlayer wedge sites including FES). Protonation−deprotonation reactions associated with the edge structure of smectites and illites—which at low solution pH can impact the adsorption mechanism—are avoided in the molecular models of FES by incorporating a unique periodic structure to represent the wedge zone of HIV. Results from energy optimizations and molecular dynamics simulations clearly demonstrate the preference of Rb^+ binding at the FES relative to Cs^+, while both cations are energetically favored in FES wedge mode rather than the vermiculite interlayer.

DOI: 10.1021/jp512824k
J. Phys. Chem. A 2015, 119, 5691−5700

AUTHOR INFORMATION

Corresponding Author

*E-mail: wcelliott@gsu.edu.

Notes

The authors declare no competing financial interest.

ACKNOWLEDGMENTS

This study was supported by the U.S. Department of Energy, Subsurface Biogeochemistry Program under contract DE-SE0001475 (Elliott) and by the U.S. Department of Energy, Office of Basic Energy Sciences, Geosciences Research Program (Cygan). L.K.Z. had additional support from the Department of Geosciences at Georgia State University in the form of a graduate teaching and research assistantship for her final year of study. Stephanie Teich-McGoldrick contributed to the large-scale MD simulations of the HIV-mica wedge models. Donald Hamelberg and Marion Wampler provided important insights and suggestions that have improved the final version of the article. Sandia National Laboratories is a multiprogram laboratory managed and operated by Sandia Corporation, a wholly owned subsidiary of Lockheed Martin Corporation, for the U.S. Department of Energy's National Nuclear Security Administration under contract DE-AC04-94AL85000.

REFERENCES

(1) Francis, C. W.; Brinkley, F. S. Preferential Adsorption of ^{137}Cs to Micaceous Minerals in Contaminated Freshwater Sediment. *Nature* **1976**, *260* (5551), 511−513.

(2) Gaudette, H. E.; Grim, R. E.; Metzger, C. F. Illite: A Model Based on Sorption Behavior of Cesium. *Am. Mineral.* **1966**, *51* (11−1), 1649−1656.

(3) Zachara, J. M.; Smith, S. C.; Liu, C. X.; McKinley, J. P.; Serne, R. J.; Gassman, P. L. Sorption of Cs^+ to Micaceous Subsurface Sediments from the Hanford Site, USA. *Geochim. Cosmochim. Acta* **2002**, *66* (2), 193−211.

(4) Elprince, A. M.; Rich, C. I.; Martens, D. C. Effect of Temperature and Hydroxy Aluminum Interlayers on Adsorption of Trace Radioactive Cesium by Sediments near Water-Cooled Nuclear Reactors. *Water Resour. Res.* **1977**, *13* (2), 375−380.

(5) Lomenick, T. F.; Tamura, T. Naturally Occurring Fixation of Cesium-137 on Sediments of Lacustrine Origin. *Soil Sci. Soc. Am. J.* **1965**, *29* (4), 383−387.

(6) Goto, M.; Rosson, R.; Elliott, W. C.; Wampler, J. M.; Serkiz, S.; Kahn, B. Interactions of Radioactive and Stable Cesium with Hydroxy-Interlayered Vermiculitic Particles in Savannah River Site Soils. *Clays Clay Miner.* **2014**, *62* (3), 161−173.

(7) Wampler, J. M.; Krogstad, E. J.; Elliott, W. C.; Kahn, B.; Kaplan, D. I. Long-Term Selective Retention of Natural Cs and Rb by Highly Weathered Coastal Plain Soils. *Environ. Sci. Technol.* **2012**, *46* (7), 3837−3843.

(8) Jackson, M. L. Interlayering of Expansible Layer Silicates in Soils by Chemical Weathering. *Clays Clay Miner.* **1962**, *11*, 29−46.

(9) Fuller, A. J.; Shaw, S.; Ward, M. B.; Haigh, S. J.; Mosselmans, J. F. W.; Peacock, C. L.; Stackhouse, S.; Dent, A. J.; Trivedi, D.; Burke, I. T. Caesium Incorporation and Retention in Illite Interlayers. *Appl. Clay Sci.* **2015**, http://dx.doi.org/10.1016/j.clay.2015.1002.1008.

(10) Brouwer, E.; Baeyens, B.; Maes, A.; Cremers, A. Cesium and Rubidium Ion Equilibria in Illite Clay. *J. Phys. Chem.* **1983**, *87* (7), 1213−1219.

(11) Cremers, A.; Elsen, A.; Depreter, P.; Maes, A. Quantitative Analysis of Radiocesium Retention in Soils. *Nature* **1988**, *335* (6187), 247−249.

(12) Sawhney, B. L. Selective Sorption and Fixation of Cations by Clay Minerals: A Review. *Clays Clay Miner.* **1972**, *20*, 93−100.

(13) Poinssot, C.; Baeyens, B.; Bradbury, M. H. Experimental and Modelling Studies of Caesium Sorption on Illite. *Geochim. Cosmochim. Acta* **1999**, *63* (19−20), 3217−3227.

(14) Rajec, R.; Šucha, V.; Eberl, D. D.; Srondon, J.; Elsass, F. Effect of Illite Particle Shape on Cesium Sorption. *Clays Clay Miner.* **1999**, *47*, 755−760.

(15) Rich, C. I.; Black, W. R. Potassium Exchange as Affected by Cation Size, pH, and Mineral Structure. *Soil Sci.* **1964**, *97* (6), 384−390.

(16) Barnhisel, R. I.; Bertsch, P. M. Chlorites and Hydroxy-Interlayered Vermiculite and Smectite. In *Minerals in Soil Environments*, 2nd ed.; Dixon, J. B., Weed, S. B., Eds.; Soil Science Society of America: Madison, WI, 1989; pp 729−788.

(17) Elliott, W. C.; Savin, S. M.; Dong, H. L.; Peacor, D. R. A Paleoclimate Interpretation Derived from Pedogenic Clay Minerals from the Piedmont Province, Virginia. *Chem. Geol.* **1997**, *142* (3−4), 201−211.

(18) Harris, W. G.; Morrone, A. A.; Coleman, S. E. Occluded Mica in Hydroxy-Interlayered Vermiculite Grains from a Highly-Weaterhed Soil. *Clays Clay Miner.* **1992**, *40* (1), 32−39.

(19) Maes, E.; Vielvoye, L.; Stone, W.; Delvaux, B. Fixation of Radiocaesium Traces in a Weathering Sequence Mica -> Vermiculite -> Hydroxy Interlayered Vermiculite. *Eur. J. Soil Sci.* **1999**, *50* (1), 107−115.

(20) Naumann, T. E.; Elliott, W. C.; Wampler, J. M. K-Ar Age Constraints on the Origin of Micaceous Minerals in Savannah River Site Soils, South Carolina, USA. *Clays Clay Miner.* **2012**, *60* (5), 496−506.

(21) Meunier, A. Soil Hydroxy-Interlayered Minerals: A Re-Interpretation of Their Crystallochemical Properties. *Clays Clay Miner.* **2007**, *55* (4), 380−388.

(22) Nakao, A.; Funakawa, S.; Kosaki, T. Hydroxy-Al Polymers Block the Frayed Edge Sites of Illitic Minerals in Acid Soils: Studies in Southwestern Japan at Various Weathering Stages. *Eur. J. Soil Sci.* **2009**, *60* (1), 127−138.

(23) Bautista-Tulin, A. T.; Inoue, K. Hydroxy-Interlayered Minerals in Japanese Soils Influenced by Eolian Deposition. *Soil Sci. Soc. Am. J.* **1997**, *61* (2), 631−640.

(24) Dion, H. M.; Romanek, C. S.; Hinton, T. G.; Bertsch, P. M. Cesium-137 in Floodplain Sediments of the Lower Three Runs Creek on the Doe Savannah River Site. *J. Radioanal. Nucl. Chem.* **2005**, *264* (2), 481−488.

(25) Zaunbrecher, L. K. The Enrichment of Stable Cesium and Rubidium in Savannah River Site Soils. Ph.D. Thesis, Georgia State University, 2013.

(26) Bostick, B. C.; Vairavamurthy, M. A.; Karthikeyan, K. G.; Chorover, J. Cesium Adsorption on Clay Minerals: An EXAFS Spectroscopic Investigation. *Environ. Sci. Technol.* **2002**, *36* (12), 2670−2676.

(27) Kogure, T.; Morimoto, K.; Tamura, K.; Sato, H.; Yamagishi, A. XRD and HRTEM Evidence for Fixation of Cesium Ions in Vermiculite Clay. *Chem. Lett.* **2012**, *41* (4), 380−382.

(28) Fan, Q. H.; Tanaka, M.; Tanaka, K.; Sakaguchi, A.; Takahashi, Y. An EXAFS Study on the Effects of Natural Organic Matter and the Expandability of Clay Minerals on Cesium Adsorption and Mobility. *Geochim. Cosmochim. Acta* **2014**, *135*, 49−65.

(29) Fan, Q. H.; Yamaguchi, N.; Tanaka, M.; Tsudada, H.; Takahashi, Y. Relationship between the Adsorption Species of Cesium and Radiocesium Interception Potential in Soils and Minerals: An EXAFS Study. *J. Environ. Radioact.* **2014**, *138*, 92−100.

(30) Greathouse, J. A.; Cygan, R. T. Molecular Dynamics Simulation of Uranyl(VI) Adsorption Equilibria onto an External Montmorillonite Surface. *Phys. Chem. Chem. Phys.* **2005**, *7* (20), 3580−3586.

(31) Greathouse, J. A.; Cygan, R. T. Water Structure and Aqueous Uranyl(VI) Adsorption Equilibria onto External Surfaces of Beidellite, Montmorillonite, and Pyrophyllite: Results from Molecular Simulations. *Environ. Sci. Technol.* **2006**, *40* (12), 3865−3871.

DOI: 10.1021/jp512824k
J. Phys. Chem. A 2015, 119, 5691−5700

(32) Vasconcelos, I. F.; Bunker, B. A.; Cygan, R. T. Molecular Dynamics Modeling of Ion Adsorption to the Basal Surfaces of Kaolinite. *J. Phys. Chem. C* **2007**, *111* (18), 6753−6762.
(33) Lee, J. H.; Guggenheim, S. Single Crystal X-Ray Refinement of Pyrophyllite-1*Tc*. *Am. Mineral.* **1981**, *66* (3−4), 350−357.
(34) Brigatti, M. F.; Guggenheim, S. Mica Crystal Chemistry and the Influence of Pressure, Temperature, and Solid Solution on Atomistic Models. In *Micas: Crystal Chemistry and Metamorphic Petrology*; Mottan, A., Sassi, F. P., Thompson, J. B., Guggenheim, S., Eds.; Mineralogical Society of America: Washington, DC, 2002; Vol. *46*; pp 1−97.
(35) Loewenstein, W. The Distribution of Aluminum in the Tetrahedra of Silicates and Aluminates. *Am. Mineral.* **1954**, *39* (1−2), 92−96.
(36) Brown, G. The Dioctahderal Analogue of Vermiculite. *Clay Miner.* **1953**, *2*, 64−70.
(37) Teich-McGoldrick, S. L.; Greathouse, J. A.; Cygan, R. T. Molecular Dynamics Simulations of Structural and Mechanical Properties of Muscovite: Pressure and Temperature Effects. *J. Phys. Chem. C* **2012**, *116* (28), 15099−15107.
(38) Plimpton, S. Fast Parallel Algorithms for Short-Range Molecular Dynamics. *J. Comput. Phys.* **1995**, *117* (1), 1−19.
(39) Plimpton, S.; Hendrickson, B. A New Parallel Method for Molecular Dynamics Simulation of Macromolecular Systems. *J. Comput. Chem.* **1996**, *17* (3), 326−337.
(40) *Accelrys Materials Studio*, Release 7.0; Accelrys Software Inc.: San Diego, 2013.
(41) Cygan, R. T.; Liang, J.-J.; Kalinichev, A. G. Molecular Models of Hydroxide, Oxyhydroxide, and Clay Phases and the Development of a General Force Field. *J. Phys. Chem. B* **2004**, *108* (4), 1255−1266.
(42) Berendsen, H. J. C.; Postma, J. P. M.; van Gunsteren, W. F.; Hermans, J. Interaction Models for Water in Relation to Protein Hydration. In *Intermolecular Forces*; Pullman, B., Ed.; D. Reidel: Dordrecht, The Netherlands, 1981; pp 331−342.
(43) Smith, D. E.; Dang, L. X. Computer Simulations of NaCl Association in Polarizable Water. *J. Chem. Phys.* **1994**, *100*, 3757−3766.
(44) Åqvist, J. Ion-Water Interaction Potentials Derived from Free Energy Perturbation Simulations. *J. Phys. Chem.* **1990**, *94*, 8021−8024.
(45) *Crystal Structure of Clay Minerals and Their X-Ray Identification*; Brindley, G. W., Brown, G. C., Eds.; Mineralogical Society: London, 1980; Vol. *5*, p 495.
(46) Ewald, P. P. Die Berechnung Optishcer Und Elektrostatischer Gitterpotentiale. *Annalen der Physick* **1921**, *64*, 253−287.
(47) Tosi, M. P. Cohesion of Ionic Solids in the Born Model. *Solid State Phys.* **1964**, *131*, 533−545.
(48) Frenkel, D.; Smit, B. *Understanding Molecular Simulation*; Academic Press: San Diego, 1996.
(49) Huheey, J. E. *Inorganic Chemistry: Principles of Structure and Reactivity*; Harper and Row: New York, 1972.
(50) Fenter, P.; Lee, S. S.; Skelton, A. A.; Cummings, P. T. Direct and Quantitative Comparison of Pixelated Density Profiles with High-Resolution X-Ray Reflectivity Data. *J. Sync. Rad.* **2011**, *18*, 1−9.
(51) Burgess, J. *Ions in Solution*; Wiley and Sons: New York, 1988.
(52) Ockwig, N. W.; Cygan, R. T.; Criscenti, L. J.; Nenoff, T. M. Molecular Dynamics Studies of Nanoconfined Water in Clinoptilolite and Heulandite Zeolites. *Phys. Chem. Chem. Phys.* **2008**, *10* (6), 800−807.

DOI: 10.1021/jp512824k
J. Phys. Chem. A 2015, 119, 5691−5700